

DESIGN AND POWER CONDITIONING FOR THE COIL-GUN

Z. Zabar, Y. Naot, L. Birenbaum, E. Levi and P.N. Joshi

Polytechnic University, Weber Research Institute  
333 Jay Street, Brooklyn, NY 11201

**Abstract:** This paper describes the power conditioning scheme for a contactless coilgun called the Linear Induction Launcher (LIL) as an open-loop integrated system. The barrel of the LIL consists of a linear array of coils carrying polyphase currents. These create an electromagnetic wave packet which moves with increasing velocity from breech to muzzle, smoothly accelerating a conductive sleeve which carries a set of azimuthal currents sinusoidally distributed along its length, and which encloses the projectile payload. The power conditioner provides high utilization of energy by transferring energy from capacitor to capacitor simultaneously with the projectile movement. A modular construction of the barrel is described together with laboratory results obtained with a breadboard model of the power conditioner circuit.

INTRODUCTION

In its simplest form, the coil gun is an electromagnetic accelerator whose propulsive force is due to the interaction between two coaxial coils: a stationary driver, and a moving driven coil. The force is attractive if the currents flow in the same direction in both coils, and repulsive when they flow in opposite directions. More practical than a single drive coil is the use of a longitudinal array of coils to form a gun barrel which guides the moving coil attached to the projectile. For a unidirectional current in the moving coil, the current in each drive coil must change sign at the instant that the driven coil crosses its midplane, to prevent reversal of the thrust. To achieve this sign change, the excitation current needs to oscillate synchronously with the passage of the driven coil. The oscillating circuit is tuned approximately to the frequency corresponding to the transit time between two successive drive coils. Synchronization may be accomplished, in principle, by optical sensors which trigger the drive coil switches.

Previous workers have described the induction acceleration of single conducting rings [1,2,3,4], and of multiple-coil arrangements [1,5,6]. These acceleration schemes imply that a moving coil (or coils) is driven by a packet of energy traveling along the barrel; paper [7] describes a way to inject current into the moving coils by utilizing mechanical brushes. Another approach, used by Driga, Weldon and Woodson [8], and by Elliott [9], is to design the coil-gun as a linear induction motor, based on the model for conventional electrical machines. In the latter, the barrel is excited by rotating machines, either by employing a special variable-frequency generator, or by employing a set of constant-frequency generators. Despite the excitation problems, this method has the advantage that it can be used as a theoretical model even for a traveling packet of energy arrangement.

The coil gun described in this paper, called the Linear Induction Launcher (LIL), differs from other concepts in that it is designed to be smoothly accelerated by a traveling electromagnetic wave-packet using a capacitor power source in an unusual switching scheme. In addition, typical of induction launcher systems [8,9], it does not require contacts or guides to feed and support the projectile, and has no need for exact synchronization between the projectile and the traveling magnetic wave.

This paper outlines the design concepts of the LIL with its power conditioner.

LINEAR INDUCTION LAUNCHER - DESIGN CONCEPT

Figure 1 illustrates the arrangement of the major components of the LIL, where: A, B, and C denote the phases; 1,2...i...n denote sections of the barrel, PS1 to PSn are the power supplies for those sections, and the moving part is the projectile sleeve.

The barrel coils are given polyphase energization. This creates an electromagnetic wave packet traveling longitudinally with increasing velocity  $V_s$ , satisfying Eq. 1:

$$V_s = 2\tau f \tag{1}$$

where  $\tau$  is the pole pitch and  $f$  is the frequency of the traveling wave. Only the section of the barrel in which the projectile is located, at a given moment, is excited. The frequency of the currents in the drive coils (the same as the frequency of the traveling wave) increases from one section to the subsequent one.

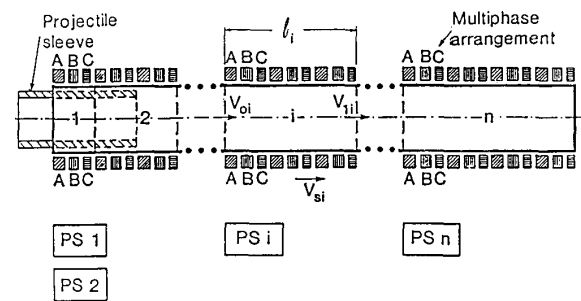


Figure 1. Modular concept of an n-section 3-phase LIL with its power conditioner.

The projectile payload is enclosed within a conductive sleeve to permit acceleration by the traveling wave packet. As long as there is a difference between the actual speed  $V$  of the projectile and the speed of the traveling wave  $V_s$ , the projectile sleeve carries induced azimuthal current, thus acting like the rotor of an asynchronous machine. The slip  $S$  between the two speeds is:

$$S = \frac{V_s - V}{V_s} \tag{2}$$

The gain in speed  $\Delta V_i$  of the projectile during its transit through section  $i$  is:

$$\Delta V_i = V_{1i} - V_{0i} = V_{si}(S_{0i} - S_{1i}) \tag{3}$$

where  $V_{0i}$  and  $V_{1i}$  are the entry and exit speeds of the section, respectively, and  $S_{0i}$  and  $S_{1i}$  are their related slips.

The length  $l_i$  of any barrel-section is proportional to the average speed of the projectile; that is:

$$l_i = \psi(S) \frac{V_{0i} + V_{1i}}{2} \quad (4)$$

where  $\psi(S)$  is a function of the entry and exit slips. Equation (4) implies that the length of the sections is not fixed: as the speed increases, the section length does also. For that reason, several starting sections may be calculated to be shorter than the projectile sleeve. In this case, it is advantageous to merge these sections. For instance, the first power supply PS1 will feed, simultaneously, sections 1 and 2 at the same frequency; and then power supply PS2 will feed the same two sections at a higher frequency.

The kinetic energy  $W_{ki}$  to be transferred to the projectile in section  $i$  is:

$$W_{ki} = M \frac{V_{1i}^2 - V_{0i}^2}{2} \quad (5)$$

where  $M$  is the total mass of the projectile.

The energy dissipated in the form of heat  $W_{hi}$  in the sleeve, in each section, is given by:

$$W_{hi} = W_{ki} \frac{S_{av,i}}{1 - S_{av,i}} \quad (6)$$

where  $S_{av,i} = (S_{0i} + S_{1i})/2$  is the average slip in each section.

Since the transit time of the projectile through the barrel is only a few milliseconds, the heat transfer into the surrounding space is negligible. Therefore, the temperature rise  $\theta$  of the sleeve will be:

$$\theta = \frac{1}{c \cdot G} \sum_{i=1}^n W_{hi} \quad (7)$$

where  $c$  is the specific heat of the sleeve material,  $G$  its weight and  $n$  is the number of sections in the barrel. The mandatory requirement that  $\theta < \theta_{melt}$ , where  $\theta_{melt}$  is the melting temperature of the projectile material, provides a criterion for a minimum  $n$ .

#### POWER CONDITIONING

A six stage diagram of one phase of the power-conditioning system [10] is shown in Fig. 2a.  $L_1, L_2 \dots$  represent the equivalent inductances of the barrel coils in each section. The resistors  $R_1, R_2 \dots$  have values that are chosen to make the energy dissipated in each one equal to the sum of the kinetic energy and the ohmic losses of the corresponding section. The initial energy is stored in the capacitors  $C_1, C_2 \dots$ . The power conditioning diagram suggests that all the power supplies of Fig. 1 are cascade-connected in order to utilize the left-over energy of the previous stage.  $CS_1 - CS_6$  are current sensors.

For the sake of clarity, assume a current swing of only half a cycle in each loop. Initially, all the capacitors are charged with alternating polarity to a voltage level of  $V_0$ , and all switches  $T_1, T_2 \dots$  are open. When the first switch  $T_1$  closes, an energy equivalent to the energy transferred to the projectile is dissipated in the resistor  $R_1$ . The left-over energy reverses the charge across the capacitor  $C_1$ . At time  $t_1$  (see Fig.2b), the instant of zero current-crossing, the

switch  $T_1$  opens and  $T_2$  closes. For this second loop, the two capacitors  $C_1$  and  $C_2$  are connected in series, generating a higher initial voltage  $\Delta V + V_0$  and a higher oscillation frequency. This process allows the energy left in  $C_1$  to be used together with the stored energy in  $C_2$  simultaneously with the movement of the projectile. The switching sequence thus continues up to the last section of the barrel.

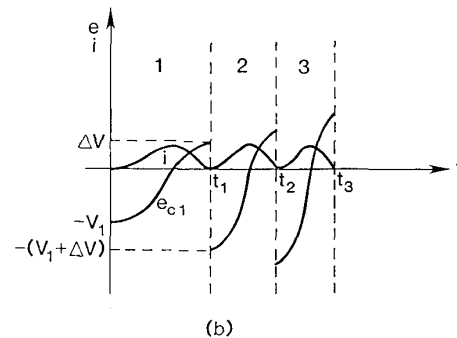
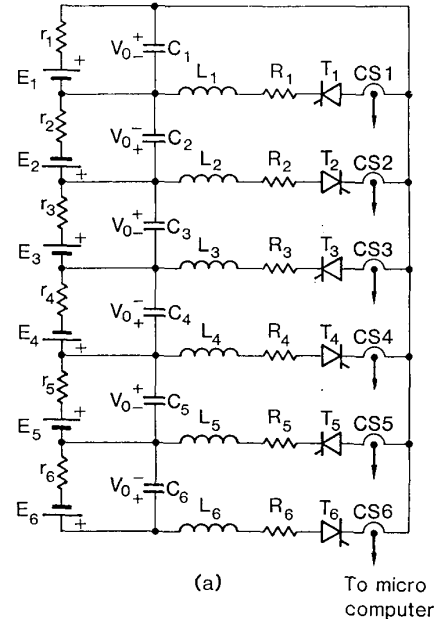


Figure 2. Six stage diagram of one phase of the power conditioner (a) equivalent circuit, (b) voltage and current waveforms.

The current  $i(t)$  in each loop has an initial value of zero, and the combined source capacitor has an initial voltage  $V_c$ . Therefore the current in each loop is given by:

$$i(t) = \frac{V_c}{\omega_d L} e^{-\alpha t} \sin(\omega_d t) \quad (8)$$

where:

$$\alpha = \frac{R}{2L}; \quad \omega_d = \sqrt{\omega_0^2 - \alpha^2} \quad \text{and} \quad \omega_0 = \frac{1}{\sqrt{LC}} \quad (9)$$

The kinetic energy  $E_k$  and the heat losses  $E_h$  in each section of the barrel can be calculated from Eqs. 5 and 6. The energy  $E_R$  dissipated in the equivalent resistor  $R$  of each is:

$$E_R = E_k + E_h = R \int_0^t i^2(t) dt \quad (10)$$

Integrating Eq. 10 for  $t = m \cdot \pi / \omega_d$ , where  $m = 1, 2, 3 \dots$ , provides the ratio  $K_m$  between the stored energy  $E_c$  in the capacitor and the dissipated energy  $E_R$ , at half-cycle intervals:

$$K_m = \frac{E_R}{E_c} = 1 - e^{-2\alpha \frac{m\pi}{\omega_d}} \quad (11)$$

The value of  $K_m$  is a function of the mutual inductance coefficient between the barrel coils and the sleeve projectile.

Solving Eq. 11 for  $\alpha$ , and using the relations in Eq. 9, one can obtain the value of the equivalent resistor  $R_i$  for each section. Since the equivalent inductance  $L_i$  is a function of barrel and sleeve dimensions, and since the frequency of each section is known (Eq. 1), one can calculate the value of  $C_i$  using Eq. 9:

$$C_i = \frac{1}{\omega_{di}^2 L_i (1 + a^2)} \quad (12)$$

where  $a = \alpha_i / \omega_{di}$ . The initial voltage  $V_{ci}$  across the capacitor of any given section:

$$V_{ci} = \sqrt{\frac{2 \cdot E_{ci}}{C_i}} \quad (13)$$

The value of the left-over voltage  $V_{cio}$  at the instant of zero-crossing of the current is:

$$V_{cio} = V_{ci} \cdot e^{-0.5\alpha m T_d} \cdot \cos(m\pi) \quad (14)$$

where  $T_d$  is the period of  $\omega_d$ . The value of the first peak of the current in the  $i$ th section can be obtained from Eq. 8:

$$I_{pi} = \frac{V_{ci}}{\omega_{di} L_i \sqrt{1 + a^2}} e^{-a \tan(1/a)} \quad (15)$$

The energy transfer coefficient,  $\eta_w$ , defined as the ratio of the kinetic energy/stored energy, is:

$$\eta_w = \frac{\frac{1}{2} M \cdot v_m^2}{\frac{1}{2} \sum_{i=1}^n C_i \cdot V_{ci}^2} \quad (16)$$

where  $n$  is the number of sections, and  $v_m$  is the muzzle velocity.  $C_i$  and  $V_{ci}$  are the values of individual capacitors and their initial voltages.

## POWER CONDITIONER EXPERIMENT

A six-stage scaled-down breadboard circuit of the power conditioner was built in the laboratory. The diagram is shown in Fig. 2a. The capacitors  $C$  were charged with alternating polarity, as shown in the figure, through individual power supplies  $E$ . The resistors  $r$ , in the power supply circuits, were chosen to make the  $rC$  time constant much larger than a period of oscillation,  $rC \gg 2\pi\sqrt{LC}$ , so that the power supply circuits did not interfere with the energy transfer during switching. The Hall-effect current-sensing devices  $CS_1$  to  $CS_6$  were used to detect the zero current crossings in order to provide timing information for the firing sequence. Each sensor provided the information on the current zero crossing point. This analog signal was digitalized by the A/D converter and fed to a microcomputer, which then supplied the firing signal to the pulse amplifier of the following stage. The first thyristor was triggered manually.

Table 1. Measured capacitor voltages at instant of firing for each stage of switching circuit (data from Fig. 3).

Capacitor:	Voltage at the start of						FINAL VOLTAGE
	1st Cycle	2nd Cycle	3rd Cycle	4th Cycle	5th Cycle	6th Cycle	
C1	100	71	87	58	76	49	78
C2		100	50	92	39	81	40
C3			100	41	92	32	91
C4				100	31	90	20
C5					100	22	93
C6						100	26
Combined:	100	171	237	291	338	374	

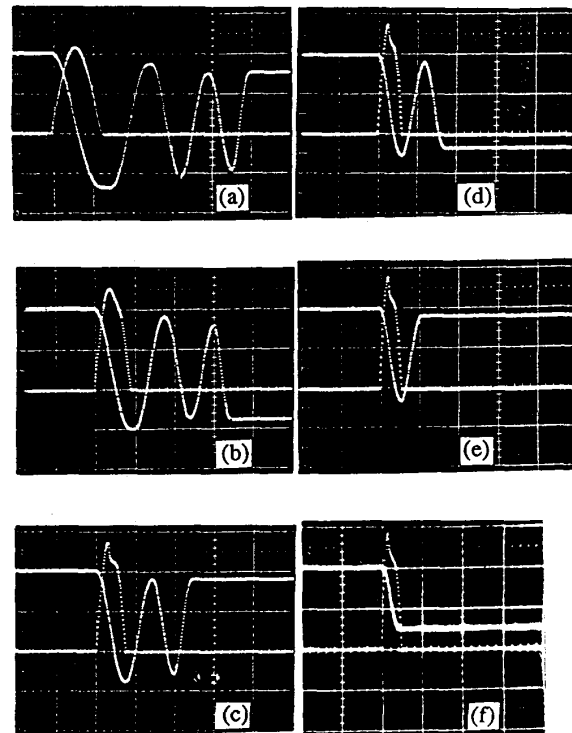


Figure 3. Oscillograms of voltage and current for six stages of switching circuit of Figure 2a. (a) - (f): Voltages across condensers  $C_1$ - $C_6$  are shown with a half-cycle of current. Scales: 10 A, 50 V, 0.5 ms/div.

In the laboratory test, the capacitors  $C$  were given equal values of  $50 \mu\text{F}$ ; the coils  $L$  and resistors  $R$  were assigned equal values  $0.8 \text{ mH}$  and  $0.8 \Omega$ , respectively. This means that the frequency  $f$  of the six stages varied from about  $f_1=800$  to  $f_2=2000 \text{ Hz}$ , where the ratio  $f_2/f_1$  is very close to the square root of the number of stages in the configuration. The power supply sections were selected to have identical values of  $r = 330 \text{ k}\Omega$  and  $E = 100 \text{ V}$ .

Table 1 summarizes the laboratory results, in which the voltages at the beginning and end of each cycle (stage) for each capacitor are listed.

The oscillograms in Fig. 3 show the voltage and current behavior of each capacitor. Figure 3a shows the voltage across the first capacitor  $C_1$  and the current in the first loop. The voltage oscillates three times, between peaks of  $+100$ ,  $-71$ ,  $+87$ ,  $-58$ ,  $+76$ ,  $-49$  and finally stays at  $+78$  volts (see also Table 1). The current peak is about  $22 \text{ A}$ . The current itself lasts half a cycle, and at the zero crossing the next stage is triggered. In Fig. 3b, the voltage across  $C_2$  oscillates 2.5 times, between  $+100$ ,  $-50$ ,  $+92$ ,  $-39$ ,  $+81$  and finally stays at  $-40$  volts (see also Table 1). The peak of the current increases to about  $25 \text{ A}$ . The other stages behave similarly, as illustrated by their oscillograms.

### SAMPLE DESIGN

A sample LIL design was prepared where the input data were:

Breech velocity - $0.2 \text{ km/s}$	Sleeve length - $20 \text{ cm}$ (4 times the pole pitch)
Muzzle velocity - $2.0 \text{ km/s}$	Sleeve diameter - $5 \text{ cm}$
Acceleration - $3 \cdot 10^4 \text{ g}$	Sleeve material - aluminum
Kinetic energy - $2.0 \text{ MJ}$	Projectile weight - $1 \text{ kg}$

The use of ten sections for the barrel will bring the maximum temperature of the aluminum sleeve to a reasonable value of  $405 \text{ }^\circ\text{C}$ . Each section is supplied by a six phase system. The total length of the barrel was calculated to be  $2.4 \text{ m}$  and the total transit time to be  $2.3 \text{ ms}$ . The length of the first three sections was calculated (see Eq. 4) to be shorter than the required six pole pitches. Therefore, they were merged. Figure 4 illustrates the power conditioner arrangement per phase for that takes into consideration the merging requirement. All switches are open except for  $S_{13}$  which is closed. At the entry of the projectile into the barrel, at a velocity of  $200 \text{ m/s}$ , switch  $S_1$  closes and current swing occurs in the first loop  $C_1$ ,  $S_1$ ,  $S_{13}$ ,  $R_1$ , and  $L_{13}$ , where  $L_{13}$  represents the equivalent inductance of all series-connected coils of one phase of the first three sections, and  $R_1$  represents the energy transferred to the projectile in the first section only. The

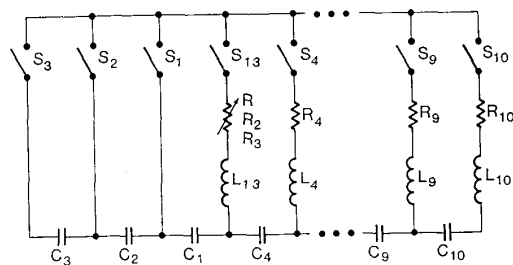


Figure 4. Power conditioner arrangement per phase for a ten section barrel with three merged sections.

current oscillation (Eq. 8) lasts for an integer number  $m$  of half cycles as dictated by the calculated transit time through the first section. At the end of the first section, switch  $S_1$  opens (at zero-crossing of the current) and  $S_2$  closes. This connects capacitors  $C_1$  and  $C_2$  in series with  $R_2$  and  $L_{13}$  and, at the same time, increases the voltage and the frequency in the second loop. At the end of the second transit time, switch  $S_2$  opens (also at zero-crossing of the current) and  $S_3$  closes. At the end of the third transit time, switch  $S_{13}$  opens, while  $S_3$  stays closed, and switch  $S_4$  closes, connecting capacitors  $C_1$ ,  $C_2$ ,  $C_3$  and  $C_4$  in series with  $R_4$  and  $L_4$ , etc.

Figure 5 shows the values of the capacitors (from Eq. 12); of the initial voltage across these capacitors (from Eq. 13); of the peak ac current in each loop (from Eq. 15); and of the total efficiency of the launcher with its power supply (from Eq. 16).

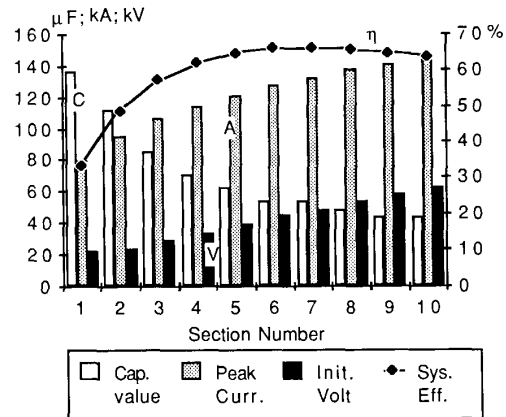


Figure 5. Capacitor values for one phase of a 6- $\Phi$  power conditioner; peak ac current in each phase loop; initial voltage across each capacitor, and the energy usage efficiency of a 10 section,  $1 \text{ kg}$  projectile,  $2 \text{ km/s}$  Linear Induction Launcher.

The energy usage efficiency (for single-shot operation) for the 10 section launcher is  $63.9\%$ . Therefore, to provide the  $2 \text{ MJ}$  kinetic energy to the projectile at the muzzle, the energy stored in the capacitors should be  $3.13 \text{ MJ}$ . The exit velocity from the first section is  $426 \text{ m/s}$ , and the muzzle velocity (exit from the tenth section) is  $2 \text{ km/s}$ . The frequency of each section is proportional to the exit velocity; the highest frequency is  $20.2 \text{ kHz}$  for the tenth section.

### CONCLUSIONS

A traveling-wave linear induction launcher (LIL), or coil-gun, in which the array of coils constituting the gun barrel is excited sequentially by a multistage power conditioner, has been described. The relatively non-impulsive, smooth accelerating force so obtained is applied to a projectile which has a conductive cylindrical outer sleeve. The barrel is divided into sections of variable length, each fed by a multiple phase system at a constant frequency. In the power conditioner of a single phase, each stage utilizes the preceding capacitor and its left-over energy to increase the voltage and the frequency of the next stage. It was demonstrated that for a ten stage configuration, the one-shot energy usage efficiency (muzzle kinetic energy/initial

stored energy in the capacitors) is above 63%. For repetitive operation, the energy stored in the capacitors can be recovered almost completely.

#### ACKNOWLEDGEMENT

This work was sponsored by SDIO/IST and managed by AFOSR under contract No. F49620-86-C-0126.

#### REFERENCES

- [1] W. S. Partridge, L. D. Harris, R. A. Davidson, J. C. Clegg, D. R. Card, and W. H. Clark "Feasibility of the Electromagnetic Accelerator", Report No. OSR-14, University of Utah; AFOSR Contract No. AF18(600)-1217, May 1957.
- [2] V. N. Bondaletov "Induction Acceleration of Conductors", Soviet Physics, Vol.12, No.2, pp 198-202, August 1967.
- [3] V. N. Bondaletov and E. N. Ivanov "Ultrahigh Axial Acceleration of Conducting Rings", Soviet Physics, Vol.22, No.2, pp 232-234, Feb. 1977.
- [4] P. Mongeau "Coaxial Air Core Electromagnetic Accelerators", Ph.D Thesis, MIT, 1981.
- [5] H. Kolm and P. Mongeau "Basic Principles of Coaxial Launch Technology", IEEE Trans. on Mag., Vol.20, No.2, pp 227-230, March 1984.
- [6] T. J. Burgess and M. Cowan "Multistage Induction Mass Accelerator", IEEE Trans. on Mag., Vol.20, No.2, pp 235-238, March 1984.
- [7] W. R. Snow, Advanced Electromagnetic Gun Design. Coilgun Final Report, Electromagnetic Launch Research, Inc., Cambridge, Mass., 1987.
- [8] M. D. Driga, W. F. Weldon, and H. H. Woodson "Electromagnetic Induction Launcher", IEEE Trans. on Mag., Vol.22, No.6, pp 1453-1458, Nov. 1986.
- [9] D. G. Elliott, "Traveling-Wave Induction Launchers," Fourth Symposium on Electromagnetic Launch Technology, University of Texas, Austin, Texas, April 12-14, 1988.
- [10] Z. Zabar and P. N. Joshi "Power Conditioner for a Coil-Gun", 6th IEEE Pulsed Power Conf., Arlington VA., June 29-July 1, 1987.